

*Supporting Information for:*

**Phenoxide-bridged Zinc(II)-Bis(dipicolylamine) Probes for Molecular Imaging of Cell Death**

Kasey J. Clear,<sup>†</sup> Kara M. Harmatys,<sup>†</sup> Douglas R. Rice,<sup>†</sup> William R. Wolter,<sup>‡</sup> Mark A. Suckow,<sup>‡</sup> Yuzhen Wang<sup>‡</sup>, Mary Rusckowski<sup>‡</sup>, and Bradley D. Smith<sup>\*,†</sup>

<sup>†</sup>*Department of Chemistry and Biochemistry, 236 Nieuwland Science Hall, University of Notre Dame, Notre Dame, Indiana 46556, United States*

<sup>‡</sup>*Freimann Life Science Center, 400 Galvin Life Science, University of Notre Dame, Notre Dame, Indiana 46556, United States*

<sup>‡</sup>*Division of Nuclear Medicine, Department of Radiology, University of Massachusetts Medical School, Worcester, MA, 01655, USA*

**Contents**

<b>A. FRET titration curves</b>	<b>S2</b>
<b>B. Aggregation and quenching of probe 2 in presence of PS-rich liposomes</b>	<b>S4</b>
<b>C. Octanol partitioning and log <i>P</i> calculation</b>	<b>S5</b>
<b>D. Cell viability data</b>	<b>S6</b>
<b>E. Additional cell microscopy and cytometry</b>	<b>S7</b>
<b>F. Animal optical imaging data and histology</b>	<b>S9</b>
<b>G. Additional radiolabeling and stability data</b>	<b>S13</b>
<b>H. NMR spectra for new compounds</b>	<b>S15</b>

## A. FRET titration curves

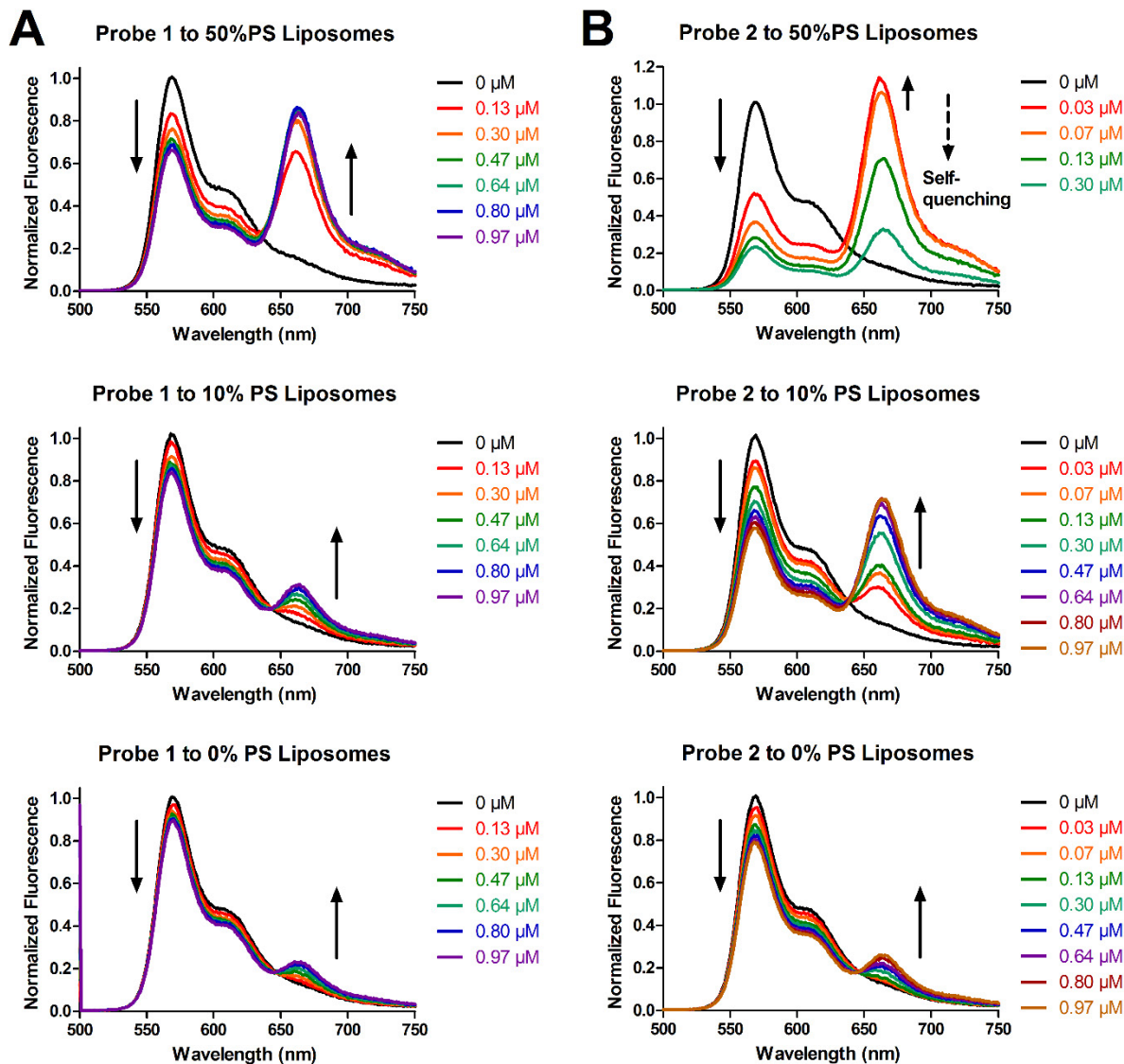


**Figure S1:** Representative fluorescence spectra for FRET titrations in response to addition of 0-1  $\mu\text{M}$  of Probe 1 (panel A) or 2 (panel B) to liposomes composed of varying amounts of POPS. Liposomes were composed of 50% PS (50:2:47:1 POPS:PEG<sub>2000</sub>DPPE:POPC:DiIc<sub>18</sub>), 10% PS (10:2:87:1 POPS:PEG<sub>2000</sub>DPPE:POPC:DiIc<sub>18</sub>), 0% PS (2:97:1 PEG<sub>2000</sub>DPPE:POPC:DiIc<sub>18</sub>). All experiments were performed in HEPES buffer (10 mM, 137 mM NaCl, 3.2 mM KCl, pH 7.4) at 25°C. Excitation was at 480 nm. Note: A loss of FRET signal at 660 nm due to self-quenching of probe 2 was observed with 50% PS liposomes (panel B, top frame).

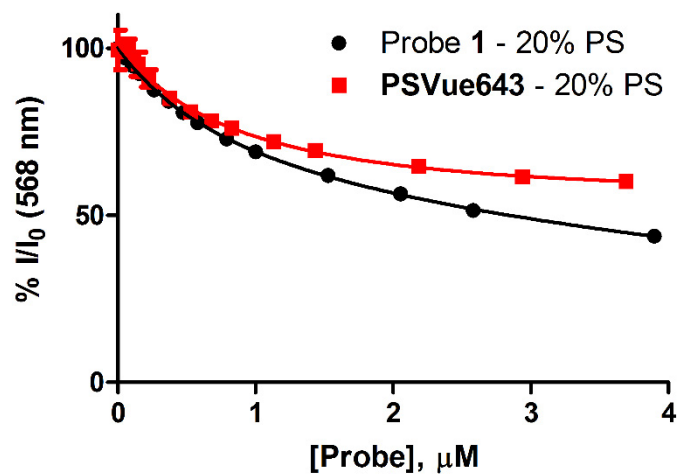


**Figure S2:** Comparison of Probe 1 and PSVue643 association with liposomes containing 20% POPS by FRET assay. See Figure 1 legend for experimental summary. Liposomes were composed of 20% PS (20:2:77:1 POPS:PEG<sub>2000</sub>DPPE:POPC:DiIC<sub>18</sub>).

## B. Aggregation and quenching of probe 2 in presence of PS-rich liposomes

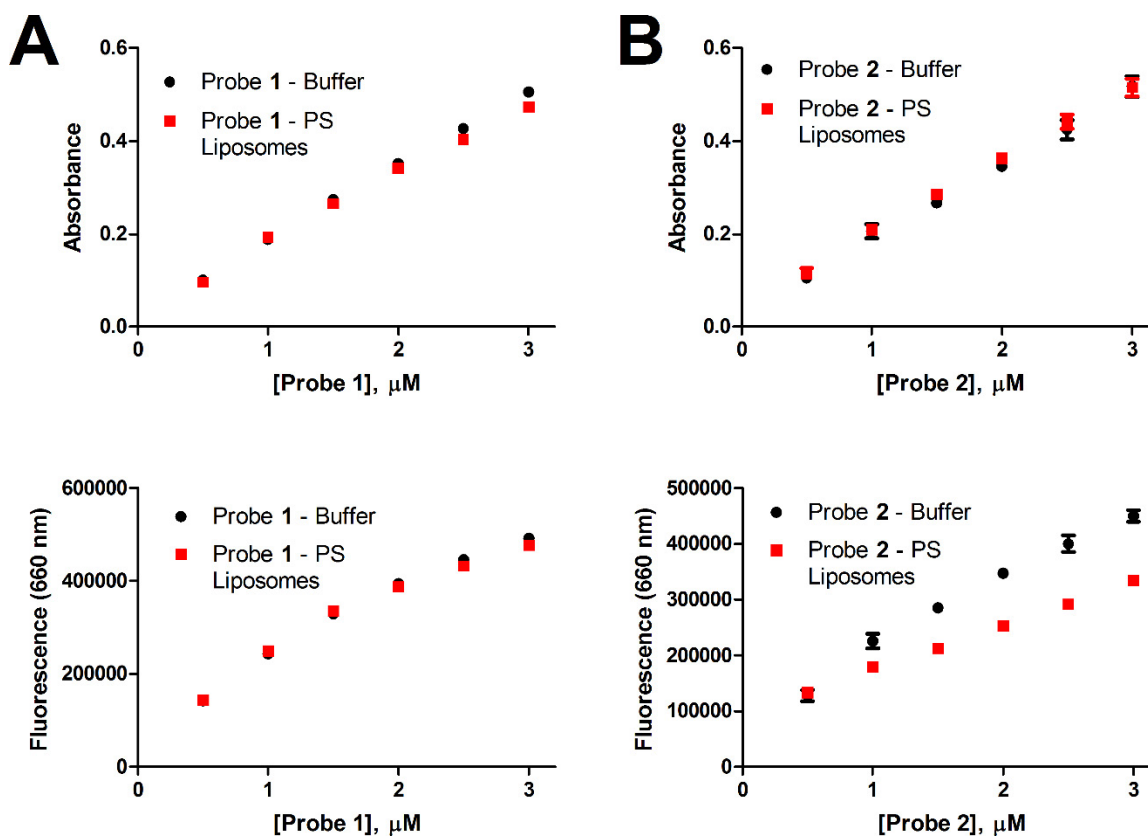
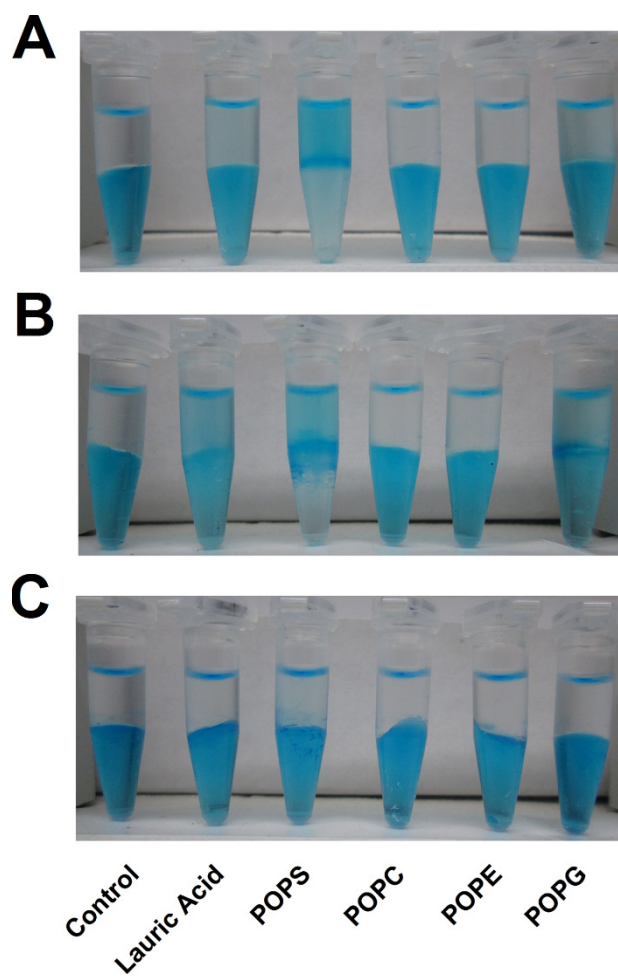


**Figure S3:** Absorbance and fluorescence changes upon addition of increasing concentrations of probe 1 (A) and 2 (B) to liposomes containing 20% POPS or buffer alone. Absorbance (644 nm, *upper*) and fluorescence (635/660 nm, *lower*) is plotted as a function of probe concentration under the two conditions. Liposomes were composed of 20% PS (20:2:78 POPS:PEG<sub>2000</sub>DPPE:POPC). All experiments were performed in HEPES buffer (10 mM, 137 mM NaCl, 3.2 mM KCl, pH 7.4) at 25°C. Probe 2 measurements are reported as the average and standard deviation of three measurements and for most points on the graphs the error bars are smaller than the symbols.

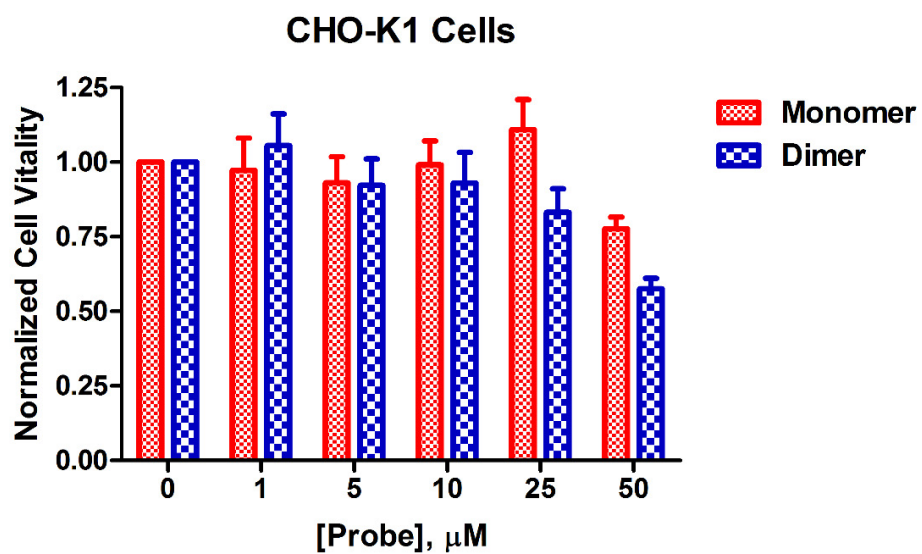
### C. Octanol partitioning and log $P$ calculation



Probe	log $P$ (25 °C)					
	Control	Lauric Acid	POPS	POPC	POPE	POPG
<b>1</b>	-2.2	-1.0	0.5	-2.0	-2.0	-1.0
<b>2</b>	-1.9	-0.4	1.0	-2.3	-1.6	-0.3
<b>PSVue643</b>	-3.0	-2.2	-1.2	-2.9	-2.8	-2.1

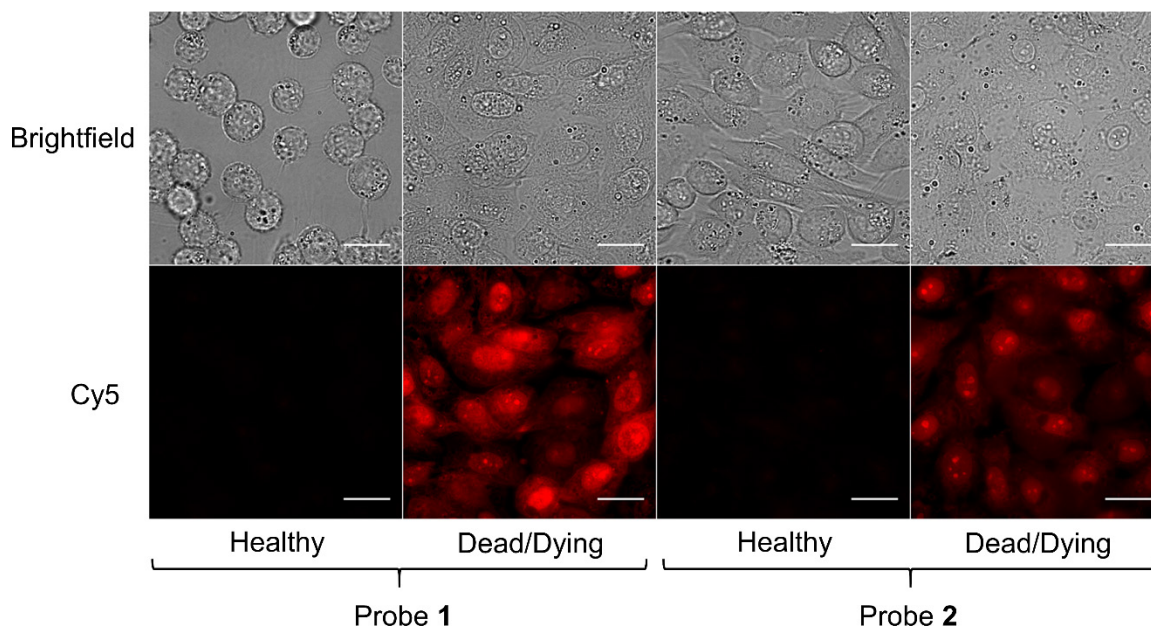
**Figure S4:** (top) Color photographs of aqueous:organic partitioning of 10  $\mu$ M probe **1** (A), **2** (B), or **PSVue643** (C) in the presence of 50  $\mu$ M lipids in 1:1 octanol:buffer. The control experiments contained no polar lipid. The aqueous layer was composed of 5 mM TES Buffer, 140 mM NaCl at pH 7.3. (lower) log  $P$  values for each probe-lipid combination calculated as indicated in Figure 3.

## D. Cell viability data

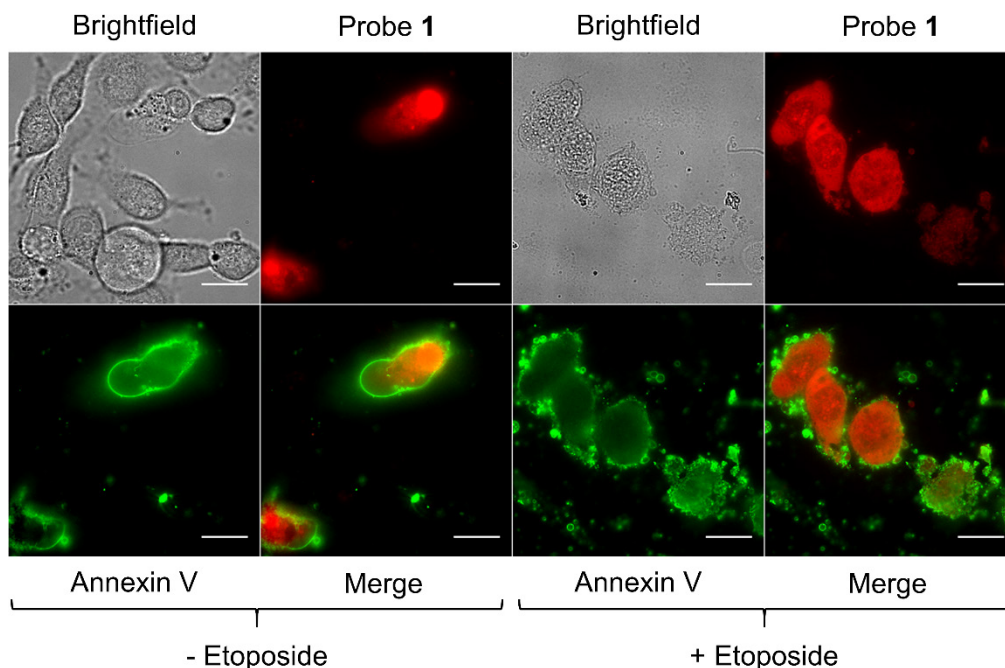


**Figure S5.** Cell viability of CHO-K1 cells treated with either **1** (red) or **2** (blue) for 18.5 h at 37 °C.

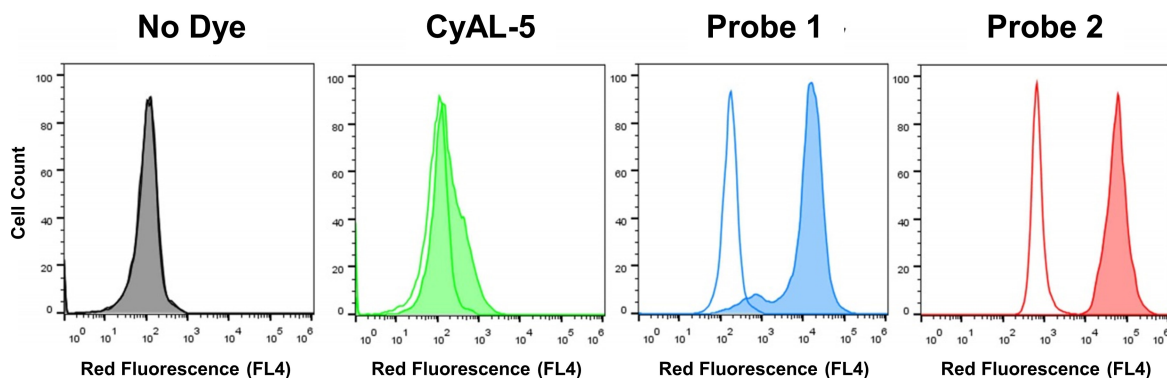
## E. Additional cell microscopy and cytometry



**Figure S6:** Fluorescence micrographs (Bright field = top; Cy5 = bottom) of healthy (A/E, C/G) or dead and dying CHO-K1 cells stained with 5  $\mu$ M of either **1** (left two panels) or **2** (right two panels). The dead and dying cells were treated with camptothecin (15  $\mu$ M) for 18 h, then incubated with 5  $\mu$ M of either probe for 15 min at 37 °C and washed with HEPES buffer. Scale bar = 25  $\mu$ m.

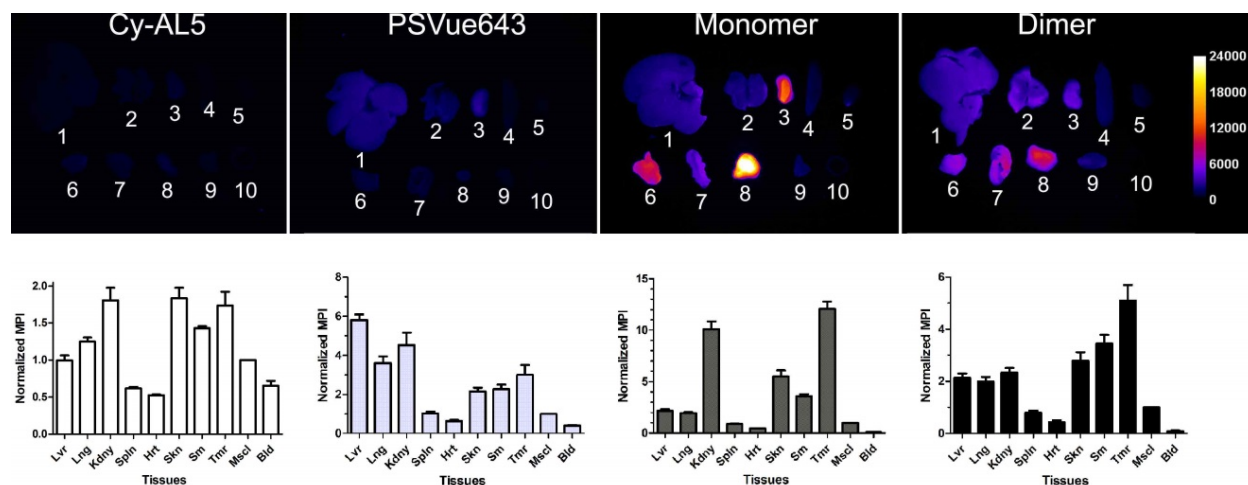


**Figure S7:** Fluorescence costaining micrographs of healthy (left) or dead and dying (right) MDA-MB-231 cells stained with 5  $\mu\text{M}$  of **1** (red fluorescence) and Annexin V-AlexaFluor480 (green fluorescence). The dead and dying cells were treated with etoposide (15  $\mu\text{M}$ ) for 6 h, then incubated with 5  $\mu\text{M}$  of **1** and Annexin V probes for 15 min and washed with HEPES buffer.

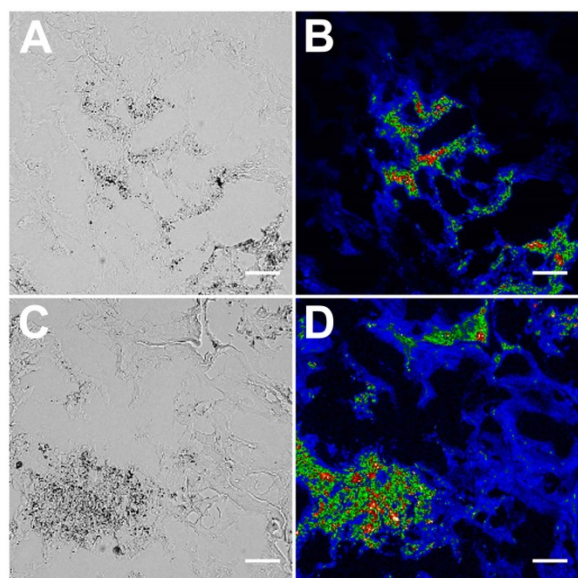


**Figure S8.** Combined histogram plot depicting flow cytometry results for different populations of CHO-K1 cells treated with 5  $\mu\text{M}$  of dye; cells left untreated (gray), cells stained with **CyAL-5** control dye (green), cells stained with monomeric probe **1** (blue), and cells stained with dimeric probe **2** (red) for 15 min in PBS (1 % DMSO). Solid-filled histograms indicate dead/dying cell populations treated prior with etoposide (15  $\mu\text{M}$ , 13 h). Unfilled histogram plots indicate healthy cell populations.

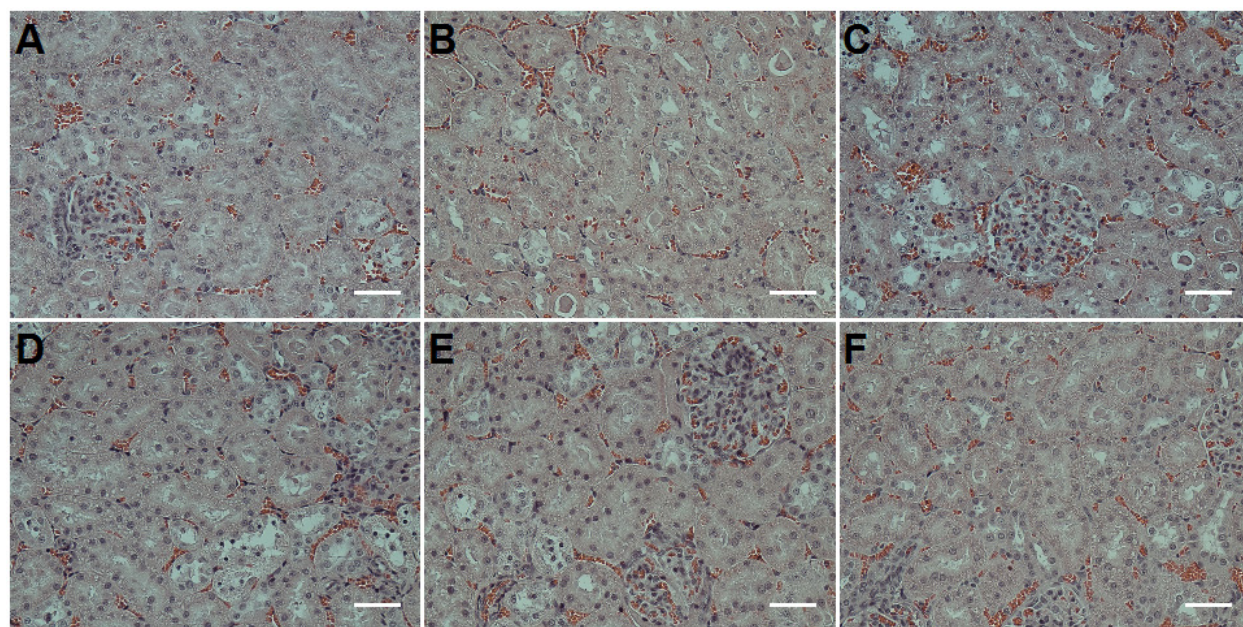
## F. Animal optical imaging data and histology



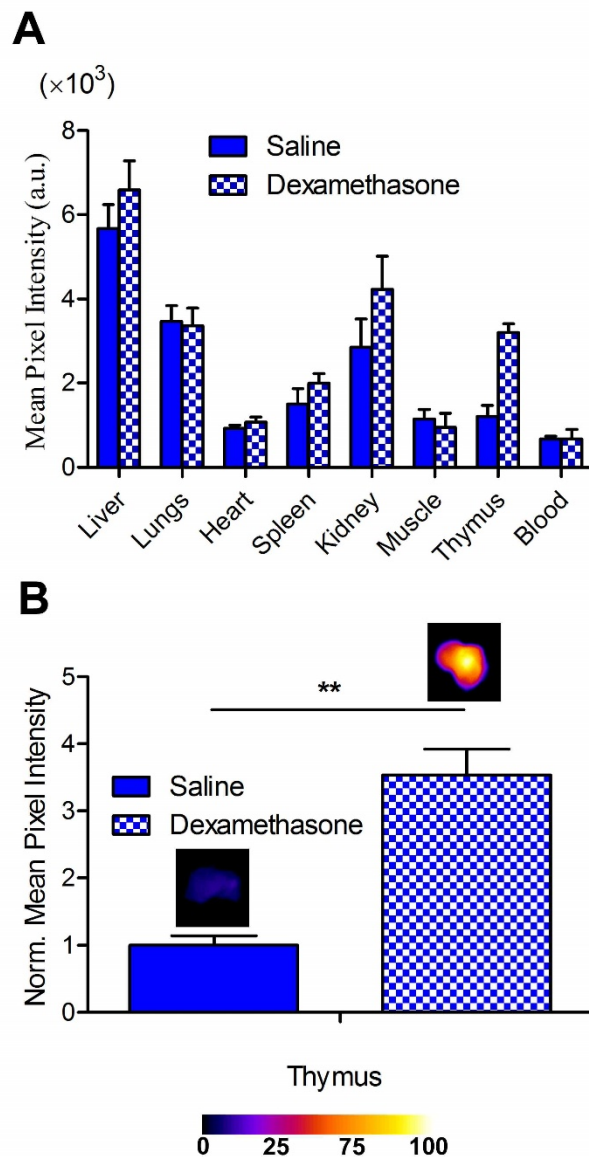
**Figure S9.** Ex vivo fluorescence images of excised organs taken from rats bearing a subcutaneous prostate tumor 24 h after intravenous dosing (150 nmol) with untargeted **CyAL-5** control dye, **PSVue643**, Monomer (1), or Dimer (2) (upper). Organs are listed as the following: 1, Liver (Lvr); 2, Lung (Lng); 3, Kidney (Kdny); 4, Spleen (Spln); 5, Heart (Hrt); 6, Skin (Skn); 7, Small Intestine (Sm); 8, Tumor (Tmr); 9, Muscle (Mscl); 10, Blood (Bld). Bar graphs showing ex vivo tissue distribution of **CyAL-5**, **PSVue643**, Monomer (1), and Dimer (2) (lower). Error bars are standard error of the mean (N = 4, 4, 10, 6, respectively of each probe) of the mean pixel intensities (MPI) normalized to muscle.



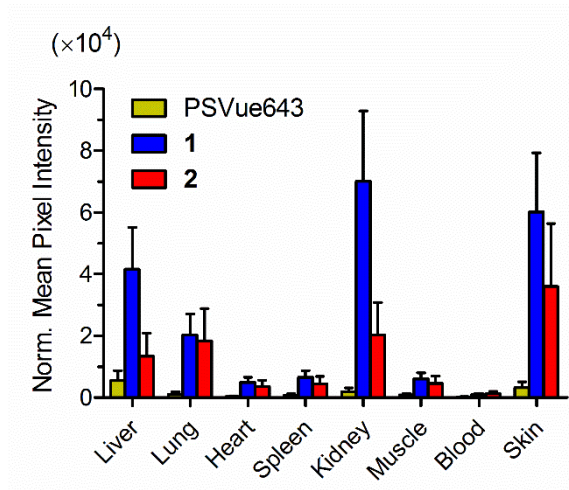
**Figure S10.** Coregistered micrographs of histological slices (5  $\mu\text{m}$ ) of tumor core from rat prostate tumor model. The brightfield images (A, C) show necrotic cells as darker regions that colocalize with deep-red fluorescence emission of **1** (B) and **2** (D). Scale bar = 130  $\mu\text{m}$



**Figure S11.** Haematoxylin/eosin staining of excised rat kidneys showing that probes do not induce cell death in the kidney. Representative histological slices of kidney from Lobund-Wistar rats that were euthanized at 24 h after intravenous injections of (A) saline, (B) **CyAL-5** control, (C) **PSVue643**, (D) **2**, and (E) **1**. The slice shown in (F) is from a rat that was euthanized 7 days after treatment with probe **1**. In each treatment, rats were injected with 150 nmol of probe. Scale bars = 50  $\mu\text{m}$ . N = 3.

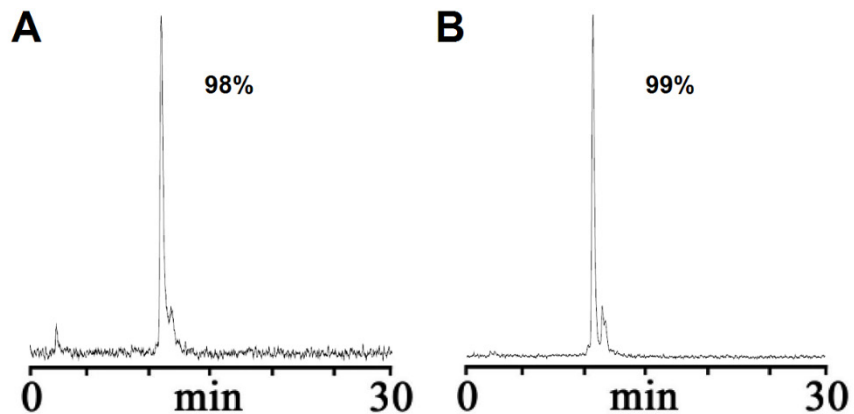


**Figure S12:** Comparison of probe **1** localization between dexamethasone and saline treatment in a thymus atrophy model of cell death in immunocompetent mice. (A) Biodistribution of **1** in excised organs taken from the saline-treated (solid blue) or dexamethasone-treated (checked blue) cohorts 3 h after intravenous dosing. (B) Mean pixel intensities for probe fluorescence in the excised thymi. Error bars are the standard error of the mean.  $N = 3$  for both cohorts.  $P$  values  $\leq 0.01$  (\*),  $\leq 0.001$  (\*\*), or  $\leq 0.0001$  (\*\*\*) are considered statistically significant. SKH1 mice were given intraperitoneal injections of dexamethasone at a dose of 50 mg/kg or saline. After 24 h, the imaging probe (10 nmol) was injected via the tail vein, and after 3 h mice were sacrificed and organs were imaged using a planar fluorescence imaging station.

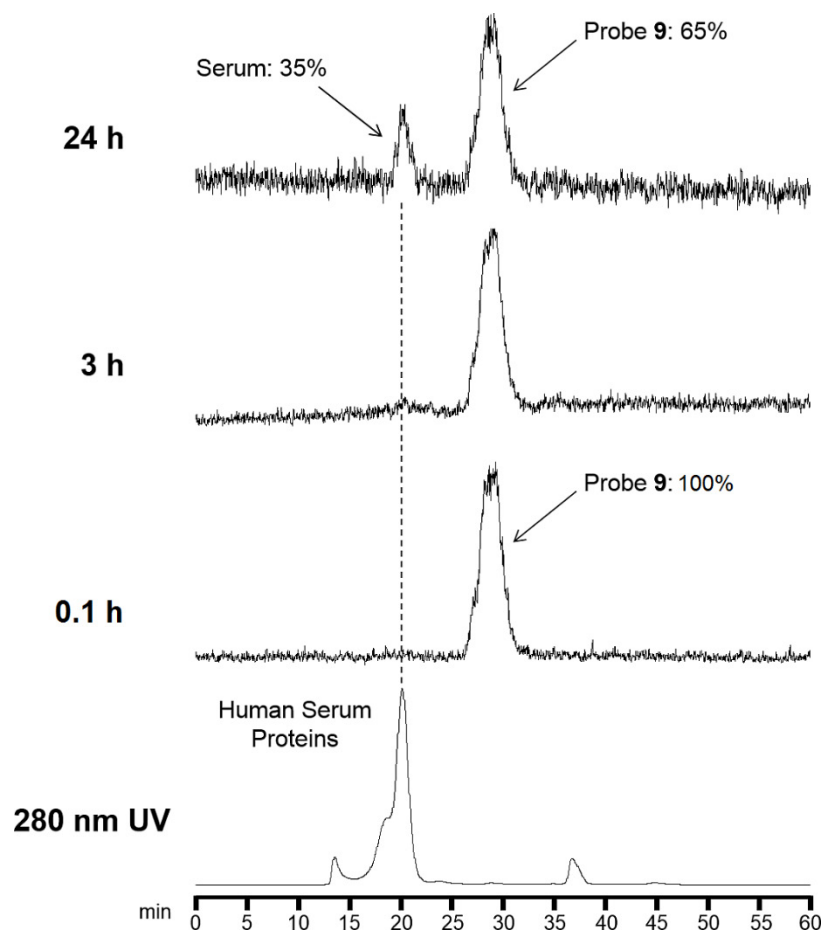


**Figure S13:** Probe localization in healthy SKH1 hairless mice 24 h after probe injection. Error bars are standard error of the mean. N = 3. Each cohort was given a retroorbital intravenous injection of fluorescent probe (20 nmol) in water (1% DMSO). The animals were euthanized 24 h later and the organ biodistributions were determined by imaging the excised tissues using a planar fluorescence imaging station with deep-red filter set.

## G. Additional radiolabeling and stability data

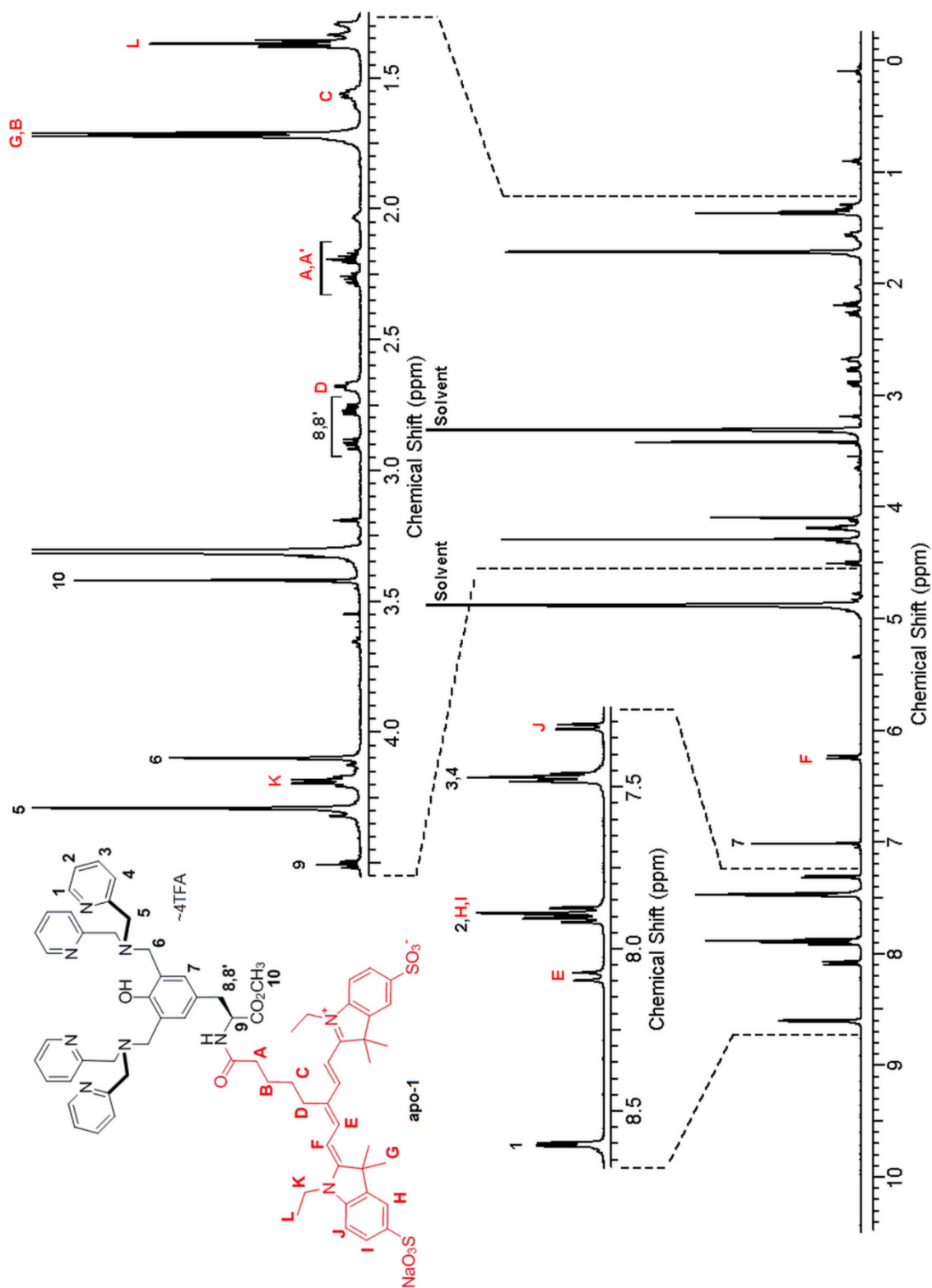


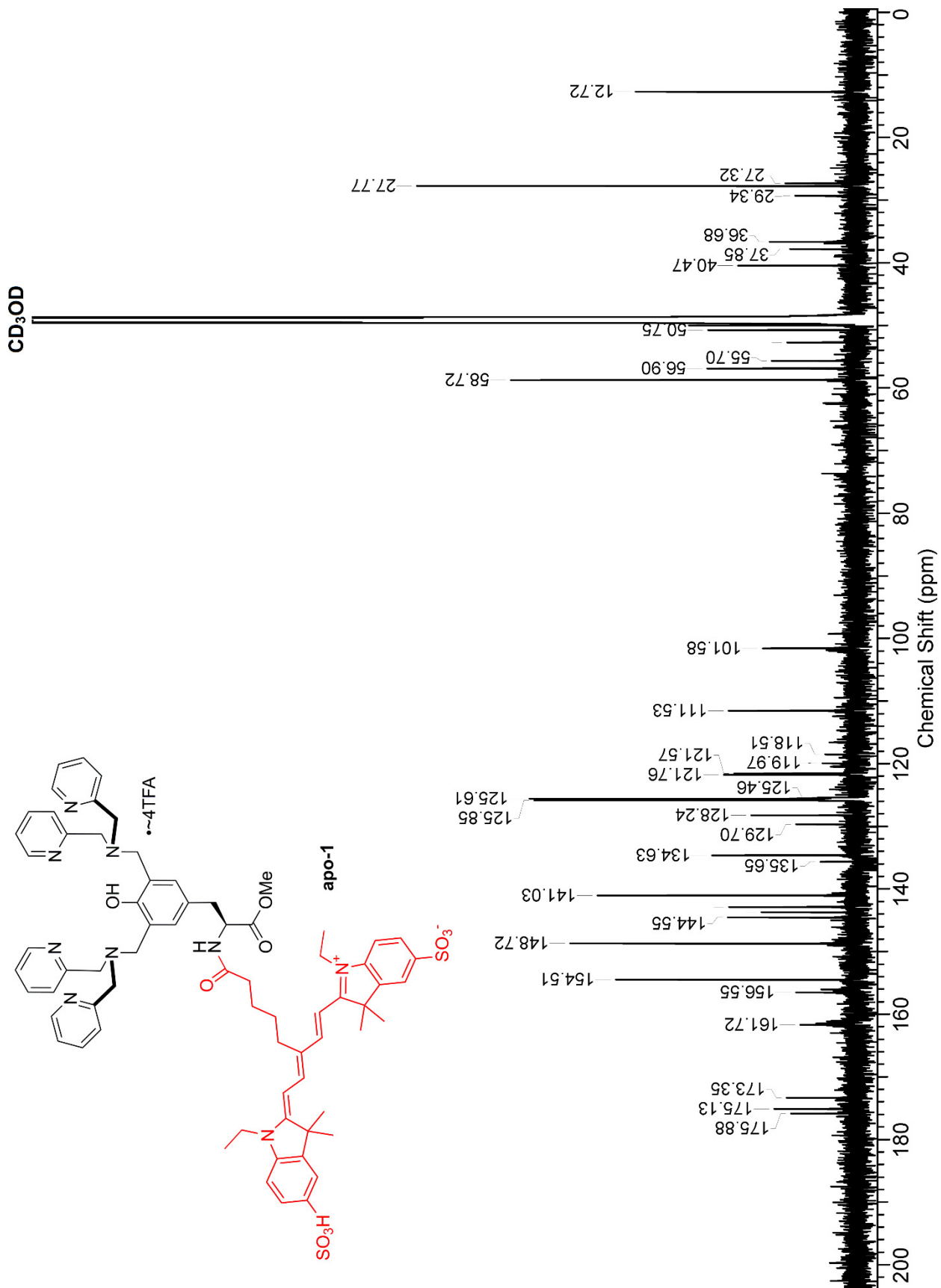
**Figure S14:** Radiopurity of **9** and **10**. HPLC radiochromatograms and radiopurities of **9** (A) and **10** (B). The retention times are 11.5 and 11.8 min, with radiopurities of 98% and 99%, respectively. The uncomplexed  $^{111}\text{In}$  eluted at ~3 min, and the tailing observed with **9** and **10** at ~12 min is an artifact of the HPLC instrument. The samples were judged pure enough for immediate animal dosing without further purification.



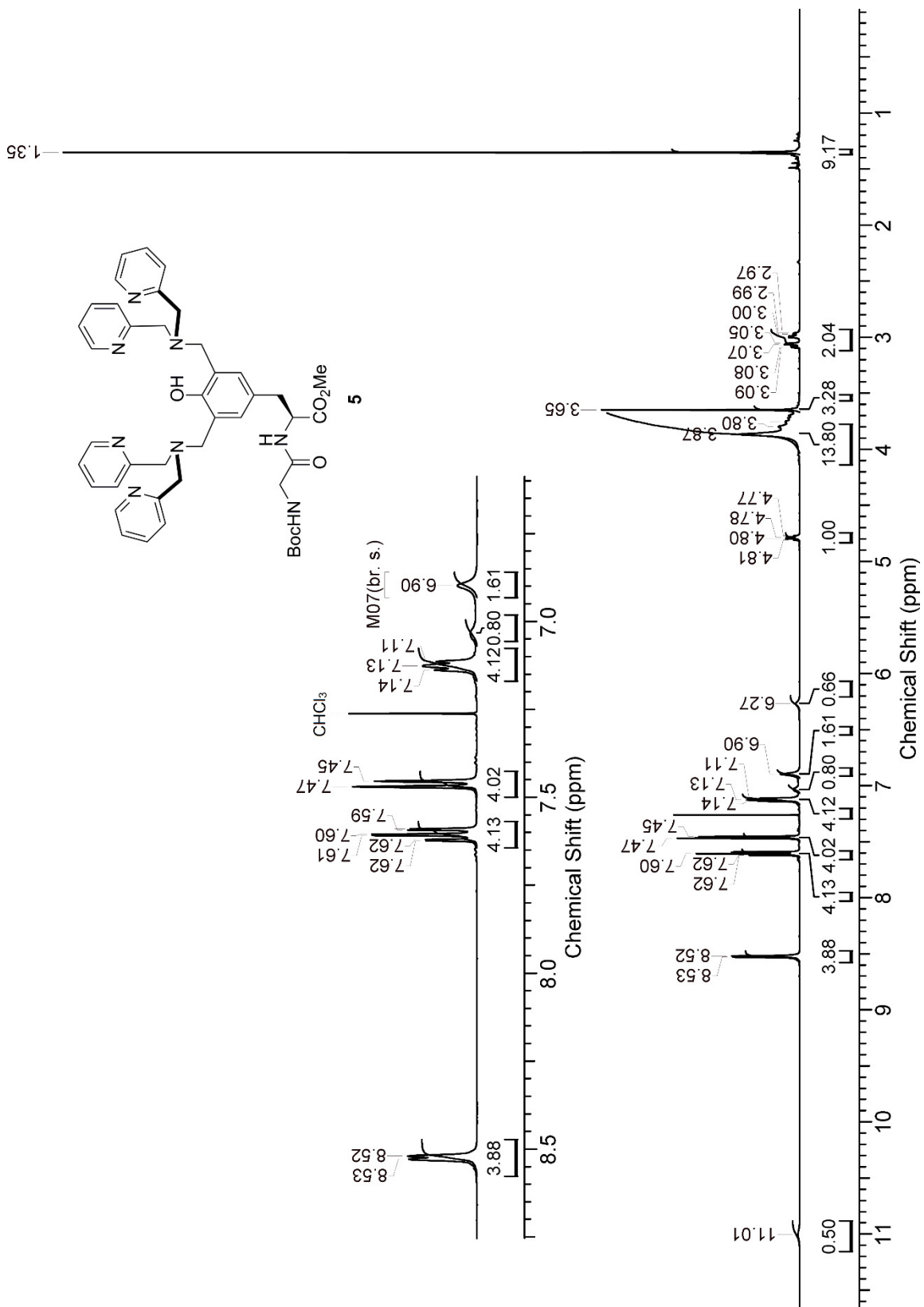
**Figure S15:** Serum stability and transfer for  $^{111}\text{In}$  complex **9**. Size exclusion HPLC ultraviolet- and radio- chromatograms of **9** mixed with human serum after incubation at 37 °C for 0 to 24 hours.

## H. $^1\text{H}/^{13}\text{C}$ NMR Spectra

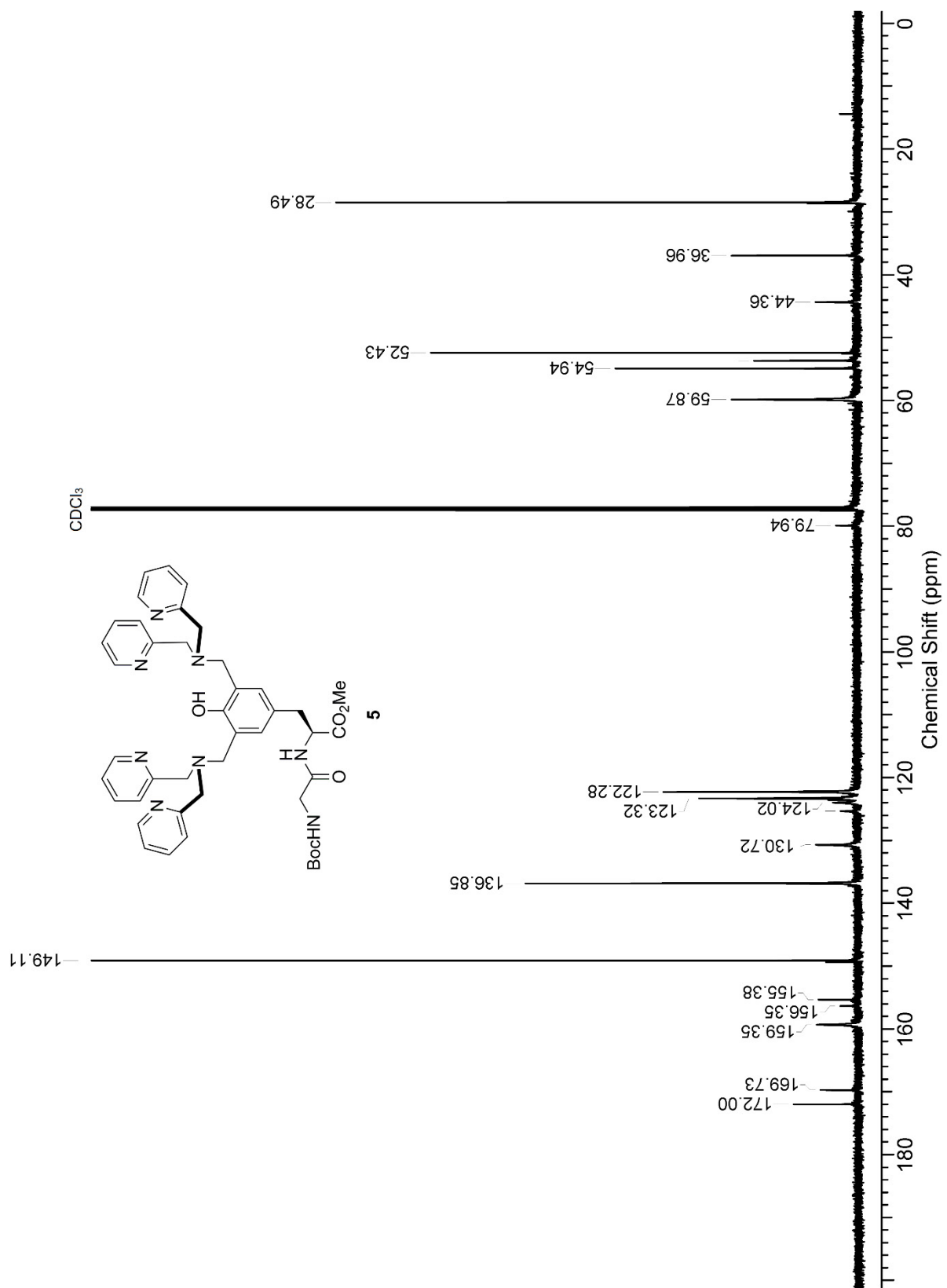


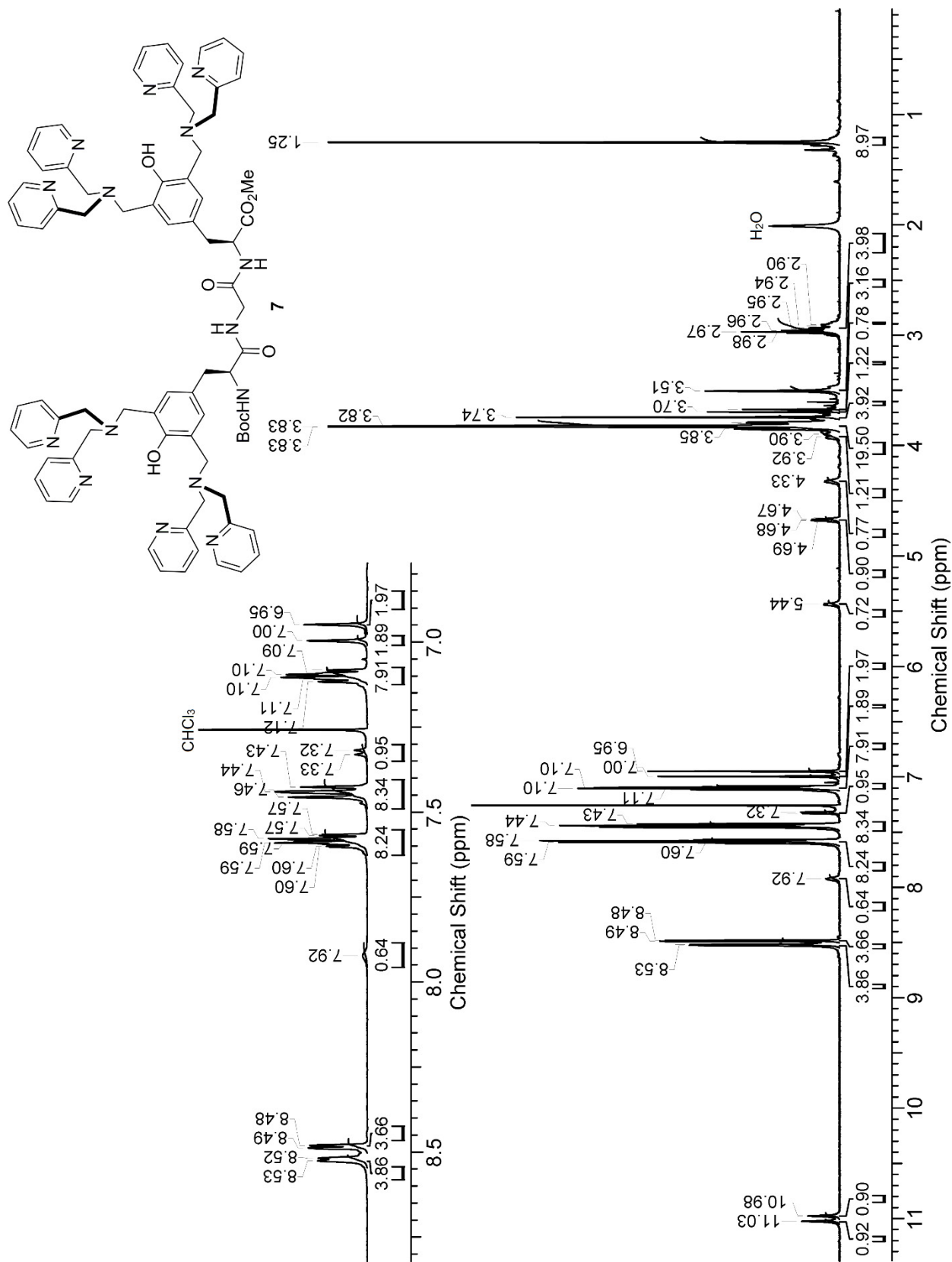


Compound apo-1 <sup>13</sup>C NMR (CD<sub>3</sub>OD, 151 MHz)



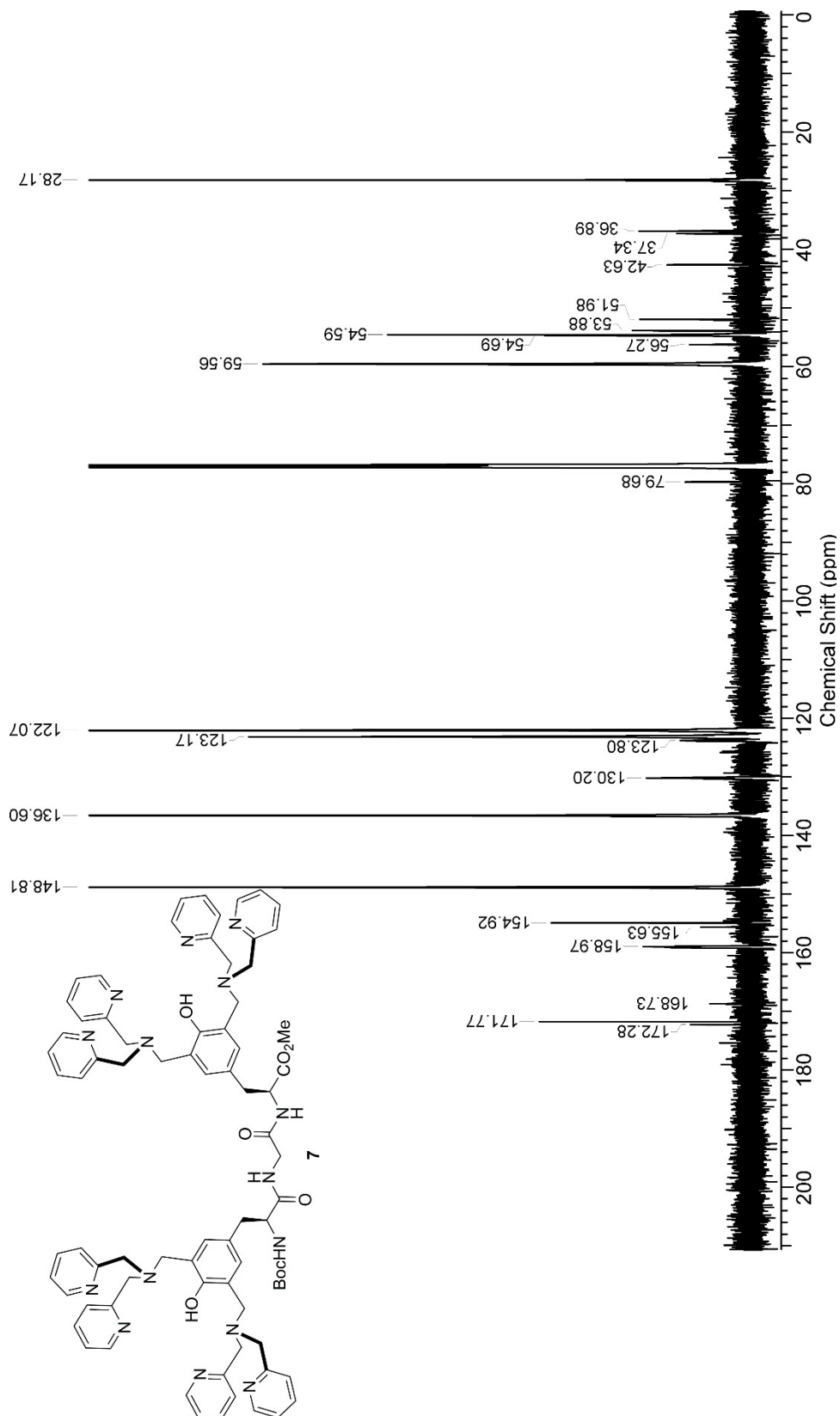
Compound 5 <sup>1</sup>H NMR (CDCl<sub>3</sub>, 500 MHz)

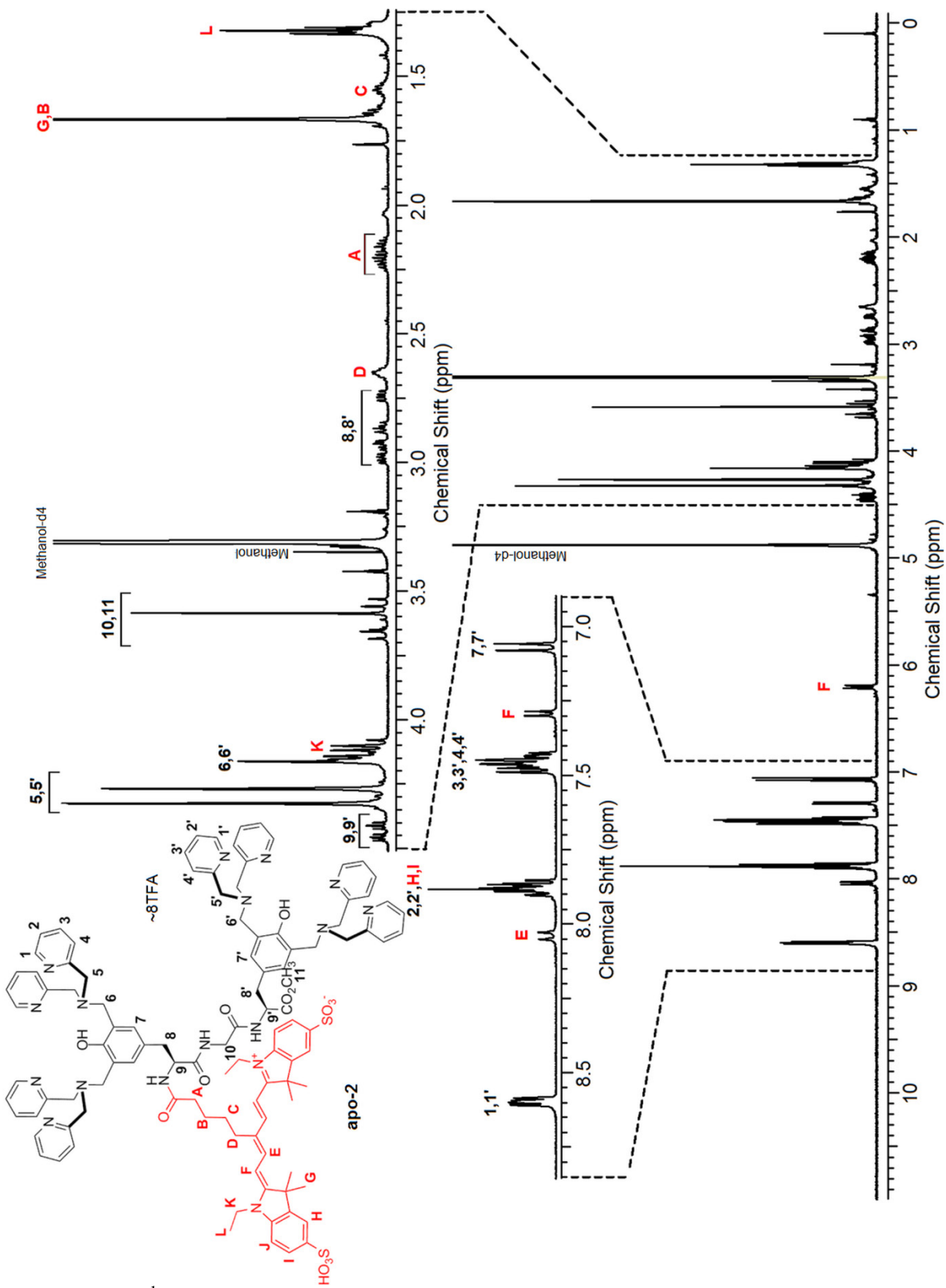




Compound 7 <sup>1</sup>H NMR (CDCl<sub>3</sub>, 500 MHz)

Compound 7  $^{13}\text{C}$  NMR ( $\text{CDCl}_3$ , 151 MHz)





Compound apo-2  $^1\text{H}$  NMR ( $\text{CD}_3\text{OD}$ , 600 MHz)

